International Journal of Nanomedicine

Dovepress
open access to scientific and medical research

Open Access Full Text Article

ORIGINAL RESEARCH

Characterization, Synthesis, and Biological Activities of Silver Nanoparticles Produced via Green Synthesis Method Using *Thymus Vulgaris* Aqueous Extract

Umer Ejaz[1], Muhammad Afzal[1], Modasrah Mazhar[1], Muhammad Riaz[1], Naveed Ahmed[2], Waleed Y Rizg[3,4], Amerh Aiad Alahmadi[4], Moutaz Y Badr[5], Rayan Y Mushtaq[6], Chan Yean Yean[2]

[1]Department of Basic and Applied Chemistry, Faculty of Science and Technology, University of Central Punjab, Lahore, 54000, Pakistan; [2]Department of Medical Microbiology and Parasitology, School of Medical Sciences, Health Campus, Universiti Sains Malaysia, Kubang Kerian, Kelantan, 16150, Malaysia; [3]Center of Innovation in Personalized Medicine (CIPM), 3D Bioprinting Unit, King Abdulaziz University, Jeddah, 21589, Saudi Arabia; [4]Department of Pharmaceutics, Faculty of Pharmacy, King Abdulaziz University, Jeddah, 21589, Saudi Arabia; [5]Department of Pharmaceutical Sciences, College of Pharmacy, Umm Al-Qura University, Makkah, 24381, Saudi Arabia; [6]Department of Pharmaceutics, College of Clinical Pharmacy, Imam Abdulrahman Bin Faisal University, Dammam, 31441, Saudi Arabia

Correspondence: Chan Yean Yean, Department of Medical Microbiology and Parasitology, School of Medical Sciences, Health Campus, Universiti Sains Malaysia, Kubang Kerian, Kelantan, 16150, Malaysia, Email yeancyn@yahoo.com; Muhammad Afzal, Department of Basic and Applied Chemistry, Faculty of Science and Technology, University of Central Punjab, Lahore, 54000, Pakistan, Email dr.afzal@ucp.edu.pk

Introduction: Silver nanoparticles (AgNPs) have been found to exhibit unique properties which show their potential to be used in various therapies. Green synthesis of AgNPs has been progressively gaining acceptance due to its cost-effectiveness and energy-efficient nature.

Objective: In the current study, aqueous extract of *Thymus vulgaris* (*T. vulgaris*) was used to synthesize the AgNPs using green synthesis techniques followed by checking the effectiveness and various biological activities of these AgNPs.

Methods: At first, the plant samples were proceeded for extraction of aqueous extracts followed by chromatography studies to measure the phenolics and flavonoids. The synthesis and characterization of AgNPs were done using green synthesis techniques and were confirmed using Fourier transform infra-red (FT-IR) spectroscopy, UV–visible spectroscopy, scanning electron microscope (SEM), zeta potential, zeta sizer and X-Ray diffraction (XRD) analysis. After confirmation of synthesized AgNPs, various biological activities were checked.

Results: The chromatography analysis detected nine compounds accounting for 100% of the total amount of plant constituents. The FT-IR, UV–vis spectra, SEM, zeta potential, zeta sizer and XRD analysis confirmed the synthesis of AgNPs and the variety of chemical components present on the surface of synthesized AgNPs in the plant extract. The antioxidant activity of AgNPs showed 92% inhibition at the concentration of at 1000 µg/mL. A greater inhibitory effect in anti-diabetic analysis was observed with synthesized AgNPs as compared to the standard AgNPs. The hemolytic activity was low, but despite low concentrations of hemolysis activity, AgNPs proved not to be toxic or biocompatible. The anti-inflammatory activity of AgNPs was observed by in-vitro and *in-vivo* approaches in range at various concentrations, while maximum inhibition occurs at 1000 µg (77.31%).

Conclusion: Our data showed that the potential biological activities of the bioactive constituents of *T. vulgaris* can be enhanced through green synthesis of AgNPs from *T. vulgaris* aqueous extracts. In addition, the current study depicted that AgNPs have good potential to cure different ailments as biogenic nano-medicine.

Keywords: nanotechnology, medicinal plants, antioxidant, anti-inflammatory, antidiabetic

Introduction

A nanomaterial is generally described as a material with at least one dimension between 1 nm and 100 nm. Material science has been dominated by nanotechnology as one of its most important fields of study.[1] Due to their high surface area-to-volume ratio compared to bulk materials, nanoparticles (NPs) are believed to have amazing physical and chemical properties. Biological, chemical, and physical methods can all be used to make NPs.[2] The use of

Received: 10 November 2023
Accepted: 9 January 2024
Published: 16 January 2024

nanotechnology for diagnosing and treating diseases at the nanoscale is specifically used in medical practice. Nanotechnology has also made significant contributions to the treatment of several diseases, including chronic heart disease, cancer, neurological disabilities, bacterial and viral infections, and diabetes.[3] The technology has also been applied to imaging and diagnostic devices, drug delivery, tissue engineering, implants, pharmaceutical therapies, and drug delivery methods.[4] Those findings demonstrated that NPs exhibit excellent physical, optical, and biological properties. They can also be used to create advanced materials with unique properties such as increased strength, increased electrical conductivity, and even enhanced antimicrobial activity.[5] A recent study examined the antimicrobial, antioxidant, antibiosis, and anticancer properties of silver NPs (AgNPs).[6] Due to these numerous properties, the use of AgNPs in biomedical applications has been rapidly increasing over recent years. Consistently, green synthesis of NPs has gained prominence due to its advantages over chemical and physical synthesis. Due to its cost-effectiveness, environmental friendliness, and absence of necessity for high pressure, high energy, and high temperature.[6] Additionally, AgNPs produced through green synthesis offer enhanced therapeutic efficacy compared to traditional methods.[7]

In several studies, AgNPs were synthesized through a variety of various plant parts, including seeds, flowers, and leaves.[8–10] As reducing, capping, and stabilizing compounds, flavonoids, terpenoids, ketones, carboxylic acids, amides, proteins, and enzymes function as secondary metabolites. Consequently, AgNPs can be bio-reduced and precipitated, which is a safe and efficient process.[11] Inflammation is a physiological process that the body uses to protect itself from injury, infection, and stress. Oxidative stress can be caused by an inflammatory response. Consequently, tumour growth may be accelerated, atherosclerosis may be exacerbated, coronary artery disease may be exacerbated, Alzheimer's disease lesions may be caused, diabetes and insulin resistance may be intensified, and cancer may be intensified.[12] Furthermore, therapeutic and antioxidant properties have been found in a variety of natural product extracts.[13]

The *Thymus vulgaris* (*T. vulgaris*), commonly known in Algeria as "Zaatar", belongs to the Lamiaceae family and grows throughout the Mediterranean region, the Middle East, Central Africa and southern Europe.[14] Throughout May to September, it blooms with white or pale pink flowers on small, oval, and coiled leaves. The *T. vulgaris* was traditionally used for snake and scorpion poisonings and burns. In conventional medicine, it has been widely used for its antimicrobial properties.[15,16] Moreover, it has been used as an antispasmodic, antiseptic, anthelmintic, diuretic, and sedative, as well as for its analgesic and anti-inflammatory properties and its antifungal properties.[17] Aside from being chemical agents of metallic salts, leaf, flower, and essential oil extracts contain amino acids, flavonoids, phenolic compounds, and terpenoids that stabilize the system.[18] Analyzing aspects such as particle distribution, size and morphology allowed for improvements and even the creation of new properties for NPs. The simplicity and environmental friendliness of plant-mediated biological synthesis have largely led to increased exposure in recent years. Large quantities of these chemicals can also be used to synthesize NPs.[19]

Plant extracts may produce well-characterized NPs and are a quick and economical alternative to synthetic methods for producing AgNPs. The aqueous extract of a *T. vulgaris* contains secondary metabolites, viz, caffeic acid, chlorogenic acid, gallic acid, quercetin, 2.5-O-Methylene-D-mannitol, xylitol and Quinoline, decahydro-1,7-dimethyl that have a key role in the production of AgNPs. The purpose of this study was to determine the biosynthesis of AgNPs extracted from *T. vulgaris* by applying green synthesis techniques. This work also integrates several isolation, purification, and optimization techniques for AgNPs. The effectiveness of AgNPs as hemolytic, anti-inflammatory, and anti-free radical scavengers as well as their access to further biological activities were also studied.

Materials and Methods

Sample Collection

Thymus vulgaris was purchased from Islamabad Nursery in Islamabad, Pakistan on 3rd August 2021. Identification of plant was made possible by the Department of Botany, University of Central Punjab, where an identification number (FOLST-21-3) was given.

Preparation of Plant Extract

After the collection, dust and visible particles were rinsed off from whole plant with tap water and distilled water and then dried in the fresh air under shade. The whole shade-dried plant was crushed and extracted with aqueous solution at room temperature. Aqueous extract was obtained by evaporating in a rotary evaporator. The whole residue was kept in airtight container at 4°C[20] and used for biochemical estimation and biological activities. A sterile environment was maintained throughout the whole experiment to ensure accuracy and efficacy.[21]

The aqueous extract yield of whole plant *T. vulgaris* was calculated using the formula:

$$\text{Extract yield}(\%) = \frac{\text{Weight of the Petri dish with extract(g)} - \text{Weight of the Petri dish(g)}}{\text{Weight of the sample used for extraction(g)}} \times 100$$

The % yield of extracting 100 grams of crude ethanolic extract from 500 grams of dried powder was 20% in 2500 mL of aqueous (1:5) ratio. In general, the great ability to extract secondary metabolites from plant sources may account for the yield of extract.[22]

Gas Chromatography- Mass Spectrometry

The aqueous plant extract was analyzed with GC-MS. In this chromatography study, phenyl and methyl polysiloxane were utilized as capillary columns in a Clarus 580 chromatography apparatus, and a Polaris Q mass spectrometer (EI 70 eV). As the carrier gas, helium was used at a rate of 1 mL/min. Between one litre of injection volume, a total of 1/75 were split. A temperature of 250°C was used for injection, and a temperature of 280°C was used for monitoring. Between 50 and 200°C, the mixture temperatures rose at a rate of 11°C/min, then 6°C/min from 200 to 240°C. A comparison was made between the spectrums of the unknown compound and those of the NIST library.[23]

HPLC Analysis of phenolics and Flavonoids

Phenolics and flavonoids in plant extract fractions were measured using an HPLC analysis. The columns utilized were shim-packed CLC ODS C-18 (5 mm diameter, 2.5 cm height, 4.6 mm diameter, 2.5cm height). The extracts were created using an aqueous extract with a 10 mg/mL concentration. 94:6 hydrogen aceto-acetate mobile phase A and pH 2.27 mobile phase B (ACN100%) were combined with 20 mL of plant extract. The various parameters were 15% to 45% B in the first 15 to 30 minutes and 100% to 45% in the final 35 to 40 minutes. The spectra of all UV–visible detectors were measured at 280nm.[24]

Silver Nanoparticle Synthesis

Fifty-millilitre solution of 0.1 M silver nitrate ($AgNO_3$) solution was prepared in a volumetric flask. Five-millilitre aqueous plant extract was added to the $AgNO_3$ solution to maintain a 1:5 ratio, and the subjected material was heated continuously at 70°C for 10 minutes, and colored solution turned black after 1.5 hours, indicating that $AgNO_3$ salt had been reduced. Centrifugation was performed at 10°C and 13,000 rpm to separate the pellet of $AgNO_3$, which was then washed three times with distilled water at a cooling temperature. As a result, AgNP powder was obtained by drying the obtained product overnight at 70°C aqueous AgNPs (aq. AgNPs).[1]

Characterization of Silver Nanoparticles

AgNP were synthesized efficiently using *T. Vulgaris*. The AgNPs can be detected by a change in color from pale yellow to colloidal dark brown. AgNP's synthesis and stability can be investigated by analyzing its UV–visible (UV-vis) spectra. The UV–vis spectrophotometer was used to determine the formation of the biosynthesized AgNPs (Shimadzu UV-2500PC Series) at 30 min, 1 h, 2 h, 3 h, 4 h, 6 h, 12 h, 24 h and was carried out at 350–700 nm range.[25] An infrared spectrometer with a resolution of 4 cm^{-1}, a Fourier transform infrared spectrometer (FT-IR), and 450–4000 cm^{-1} peak range was used to determine the characteristics of AgNPs using infrared spectroscopy. There were measurable peak values.[26]

Scanning Electron Microscope (SEM)

A scanning electron microscope (SEM) instrument (JOEL, JSM-6480A) operating at 20KV was used to analyze the surface morphology of AgNPs. Glass bottles were used to collect and screen the SEM test samples. SEM copper plates were coated with conductive resin tape after the dye was applied to their copper surfaces. Particles were distributed on the tape and coated with gold. A sonication process was conducted for 15 minutes and a centrifugation process was followed for 10 minutes at a speed of 10,000 rpm for dispersing the samples in ethanol. Afterwards, drops of AgNPs were poured onto carbon-coated copper grids and left to dry naturally. After five minutes of drying under a mercury lamp, SEM images were acquired at different magnifications.[27]

Zeta Potential and Zeta Sizer

In order to determine the surface potential and stability of AgNPs, it is useful to determine their zeta potential.[28] Using the Nano ZS-90 zeta sizer (Malvern Instruments, England), particle size, distribution, and zeta potential were determined for NPs. Before the measurements were conducted, a sample of NPs was diluted with pure water, and then sonicated for 10 minutes before being measured.[29] To describe the degree of non-uniformity of a distribution, the polydispersity index (PdI) was calculated.

X-Ray Diffraction Analysis

A powder X-ray diffractometer from STOE (Germany) was used for the XRD analysis. Cu K radiations (= 1.54 Ao), with a 2 range of 20–80° for AgNPs and 10–80° for aqueous extract of NPs, were a suitable source.[1] AgNPs' crystallite size was determined using the following Debye Scherrer's formula:

$$\text{Crystallite Size} = \frac{0.9\lambda}{\beta\cos\theta}$$

Where:

θ = scan range for analysis

β = Full width half maximum

λ = wavelength used for analysis (1.54 A°)

Redox Properties of Plant Extract AgNPs Components

Aqueous extract of AgNPs reveals its redox properties. Quantum was employed to estimate the redox properties of extracts in an aqueous medium. By using the density functional theory (DFT) approach and the GAUSSIAN09 software package, it was possible to make a quantum chemical calculation of the redox properties of molecules in the proton transfer (SET-PT) and hydrogen atom transfer (HAT) processes. All structures are optimized with DFT/B3LYP with a basis set of 6–311G on Gaussian 09W. The GAUSSIAN09 solvation model analyzes solvation effects using SMD.

Biological Activities

Antioxidant Activity (2, 2-Diphenyl-1-Picrylhydrazyl (DPPH) Method)

The current study was designed a modified version of the method used in a previous study.[30] A stable radical DPPH was used to measure AgNPs and vitamin C's free radical scavenging activity. A solution of fresh DPPH (2 mM in water) was mixed with 1 mL of different concentrations of AgNPs for 30 minutes at room temperature. The absorbance at 517 nm was determined using a spectrophotometer (Shimadzu UV-2500PC Series).[30] Based on the following formula given below, percentage (%) of inhibition of free radical scavenging activity was determined:

$$\%\ \text{of scavenging} = \frac{\text{Ac} - \text{As}}{\text{Ac}} \times 100$$

Where A = absorbance

Ac equals absorbance of control while as equals absorbance of AgNPs/vitamin C. All tests were repeated in triplicate, with the average of three measurements ± standard deviation being plotted as the merit Figure.

Anti-Diabetic Activity

An aq. AgNPs stock solution of 4 mg/mL was diluted to produce different concentrations of plant extracts in phosphate buffer. Acarbose and aq. AgNPs in volumes of 250, 500, 750, and 1000 mL were combined with 500 mL of α-amylase (0.5 mg/mL) and left to sit at room temperature for 10 minutes. Then, 500 L of a 1% starch solution was added, and the mixture was incubated for the following 10 minutes. Prior to adding the reaction mixture to 10 mL of distilled water, the reaction mixture was heated in a boiling water bath for 15 minutes.[28] The enzyme was substituted for the buffer at each concentration in order to calculate the absorbance of colored extracts at each concentration of the sample set. Calculate the absorbance at 540 nanometers.

$$\%\ \text{inhibition} = \frac{\text{Ac} - \text{As}}{\text{Ac}} \times 100$$

where A = Absorbance

Hemolytic Activity

By using the hemolysis test, Aq. AgNPs were assessed for their effect on red blood cells (RBCs). The RBCs are obtained from healthy young adults aged 24–30. Centrifugation at 1500 rpm for 10 minutes and subsequent washing with normal saline produced clean pellets from the blood sample. A 10% v/v solution of normal saline was utilized to suspend the obtained RBCs. Each concentration (200, 500, 750, and 1000 μg/mL^{-1}) of aq. AgNPs were incubated with RBC suspension at a ratio of 1:1 for 60 minutes, centrifuged at 5000 rpm for 5 minutes, then incubated at 37°C for 60 minutes. Using a microplate reader, absorbance was measured at 540 nm using 100 μL of the supernatant of samples.[31] The percentage of hemolysis of RBCs was calculated using this equation:

$$\text{Percentage of hemolysis}\% = \frac{\text{Sample absorbance} - \text{Negative control absorbance}}{\text{Positive control absorbance} - \text{Negative control absorbance}} \times 100$$

In-Vitro Inflammation Activity

To investigate the impact of anti-inflammatory activity, a method from previous study was used with certain modifications.[32] Each fraction of 250, 500, 750 and 1000 μg/mL was prepared at different concentrations, and 100 μL of the sample was centrifuged with 0.5 mL of bovine serum albumin BSA included. The enzyme-linked immunosorbent assay (ELISA) plates were incubated for 20 minutes at 37°C and then for 10 minutes at 70°C. A 630 nm ELISA reader was used to read ELISA plates after they had cooled down. By using the given formula, we were able to determine the percentage inhibition.[32] Diclofenac sodium at concentrations of 250,500,750 and 1000 μg/mL as a reference drug was used and treated similarly for determination of absorbance. Diclofenac sodium was used as a reference drug, and the amount was administered at 250, 500, 750, and 1000 mg/mL for the determination of absorbance, respectively.

$$\%\ \text{BSA inhibition} = \left(\text{A}_{\text{control}} - \text{A}_{\text{sample}} / \text{A}_{\text{control}}\right) \times 100$$

Here, A = Absorbance

In-Vivo Anti-Inflammatory

To induce edema in the right hind paws of rats, subcutaneous injections of 1% whey product were administered. According to the first and second groups, aqueous extract (50 grams per kilogram) and AgNPs (1 μg kg^{-1}) were administered one hour before carrageenan injections, approximately one hour before the injection of carrageenan. As a control group, only the vehicle was delivered to the third group. Diclofenac (50 μg kg^{-1}) was administered to the fourth group (standard) by means of a vernier calliper. The dose of diclofenac (50 kg^{-1}) was determined by the results of previous studies. Water vernier callipers were used to measure paw volume prior to the injection of carrageenan.[33] The volume of the inflammatory paw increased within one hour of the injection of carrageenan, three hours and five hours after the injection. As a result of the treatment, edema was inhibited in treated animals as compared to control animals using a formula:

$$\text{Inhibition}\,(\%)=(D_0-D_t)/D_0\times 100$$

In this case, D is the diameter of the injected paw, while D_0 represents the average inflammation (hind paw edema) in the control group of rats at a given point in time; and D_t represents the size of the drug-treated (ie, test or standard) rats at that point in time.

Results

Gas Chromatography-Mass Spectrometry

An analysis of the chemical nature of aqueous plant extract was conducted using GC-MS. Nine compounds account for 100% of the total amount of constituents detected in this GC-MS chromatogram as shown in Table 1 and Figure 1.

High-Performance Liquid Chromatography

The *T. vulgaris* aqueous plant extract analysis was conducted through high-performance liquid chromatography and was conducted to determine and separate its phenolic and flavonoid content. Table 2 shows the bioactive compounds derived from HPLC, including phenolics and flavonoids.

Formation of Silver Nanoparticles

The presence of AgNPs can be confirmed primarily through a change in color as a result of the reduction of $AgNO_3$ to AgNPs using the aqueous plant extract. *Thymus vulgaris* extract changed $AgNO_3$'s color from brown to dark brown when added to $AgNO_3$. The AgNPs were formed after 4 hours of incubation due to a change in solution color from light brown to dark brown. It is important to note that as the incubation time progressed, the color intensity increased, confirming an increase in the synthesis of AgNPs and a reduction in the concentration of Ag^+ ions. Due to the formation of NPs of silver in the mixture, there is a distinct color change in the mixture.[34] The formation of AgNPs, as first indicated by the change in color, was found to be at a concentration ratio of 1:4. Dark brown color was found in the concentrations of $AgNO_3$ at 2 mM.

Characterization of Silver Nanoparticles

The synthesis of AgNPs was confirmed, and it was found that the variety of chemical components present on the surface of synthesized NPs in the plant extract.

Table 1 Bioactive Compounds Identified from Aqueous Plant Extract by Gas Chromatography–Mass Spectrometry Analysis

Serial Number	Peak	Retention Time (Minutes)	Percentage Area (%)
1	4-tert-Butylphenol, TMS derivative	5.031	44.14
2	Xylitol	5.678	6.44
3	Tris (tert-butyldimethylsilyloxy)	8.583	4.66
4	7,7,9,9,11,11-Hexamethyl-3,6,8,1	9.150	5.93
5	Quinoline, decahydro-1-methyl	9.348	4.76
6	Benzamide, 2-chloro-4-trifluorom	9.845	2.77
7	2,5-O-Methylene-D-mannitol	10.230	15.53
8	Quinoline, decahydro-1,7-dimethyl-	12.017	14.39

Notes: TMS, Trimethyl[4-(1,1,3,3,-tetramethylbutyl) phenoxy]silane; Phenol, 4-tert.-octyl.

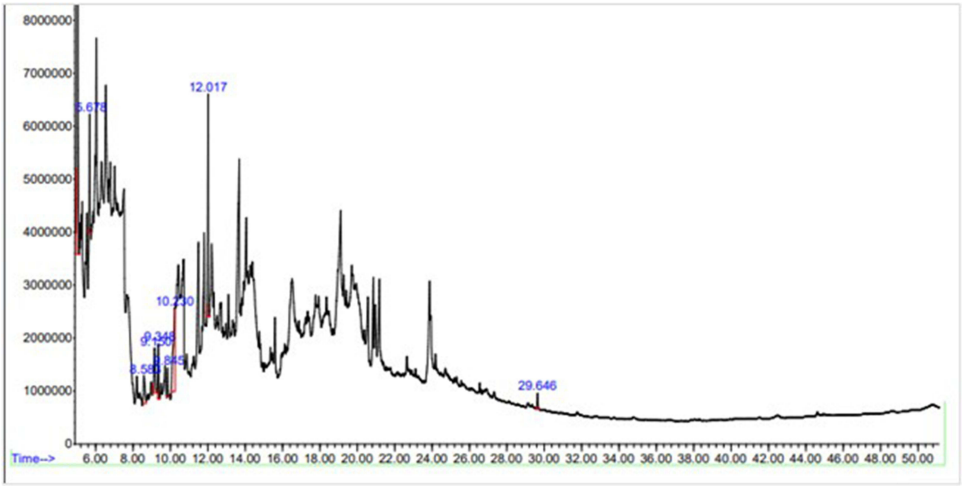

Figure 1 Gas Chromatography-Mass Spectrometry analysis. Nine compounds account for 100% of the total amount of constituents detected in this GC-MS.

UV-Visible Spectroscopy

According to Figure 2, the UV–visible spectrum of colloidal AgNPs solution formed by using 3 mM $AgNO_3$ showed a sharp peak at 400 nm. As a result, it was revealed that the form of AgNPs reduced by *T. vulgaris* extract was spherical and dispersed indicating that the peak of absorption was narrow. A single peak from surface plasmon resonance confirmed that *T. vulgaris* extract reduces silver ions and converts them to AgNPs.

Fourier Transform Infra-Red Spectroscopy

The FT-IR analysis was performed to check the presence of functional groups on order to support the HPLC results. Both plant extract and green-synthesized AgNPs displayed peaks of different intensities (Figure 3). In the FTIR spectrum of plant AgNPs, several peaks were observed at 2930.94 cm^{-1} and 1736.52 cm^{-1} indicating multiple stretches of functional groups. Carboxylic acid is the compound class O-H associated with the stretching band at 3216 cm^{-1}. The C=O stretching bands show characteristic peaks at 1736.52 cm^{-1}. Aqueous extract of *T. vulgaris* AgNPs shows the presence of functional groups such as hydroxyl (OH), phenol, C-O-C, C-H, C-S, cycloalkane, and C-Br that are shown in FT-IR spectra (Figure 3).

Scanning Electron Microscopy (SEM)

Micrographs were obtained using scanning electron microscopes at magnifications of almost 200,000 and 50,000. Biologically synthesized AgNPs were suspended in an aqueous suspension and micro-graphed by drop coating. Shaped as spheres and uniformly distributed NPs, they are shown in Figure 4.

Table 2 Quantification of Different Polyphenols Compounds (Ppm) of Aqueous Plant Extract *T. Vulgaris*. Table Shows the Phenolic and Flavonoids

Sr No.	Phytochemicals	Concentration (mg/g)	Retention Time (Minutes)
1	Phenolics		
	Gallic acid	0.148	7.01
2	Chlorogenic acid	0.012	9.37
3	Caffeic acid	0.176	10.36
4	Flavonoids		
	Quercetin	0.034	3.51

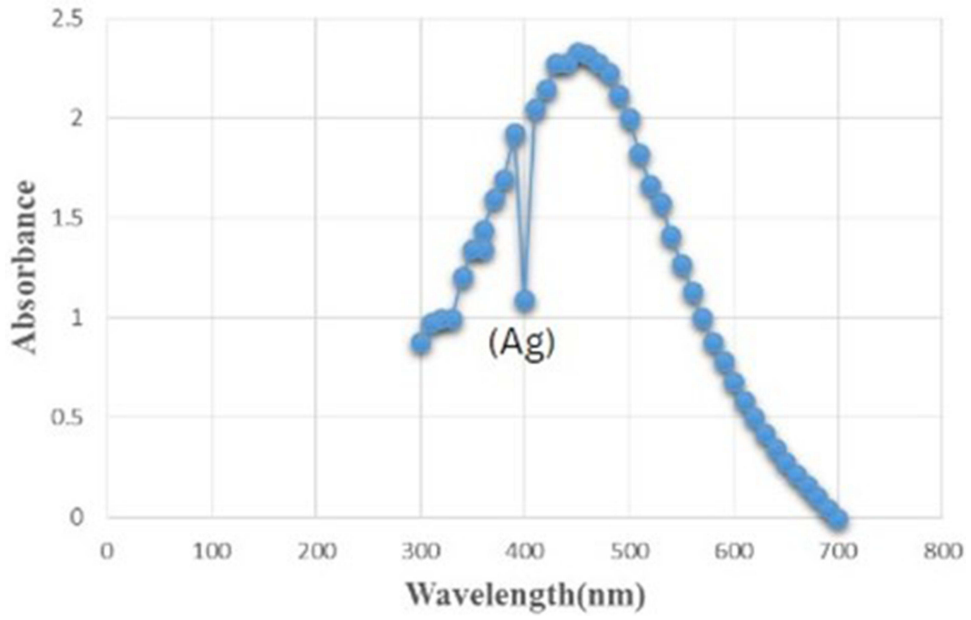

Figure 2 UV-Visible Spectra of extracted silver nanoparticles solution formed by using 3 mM $AgNO_3$ showed a sharp peak at 400 nm.

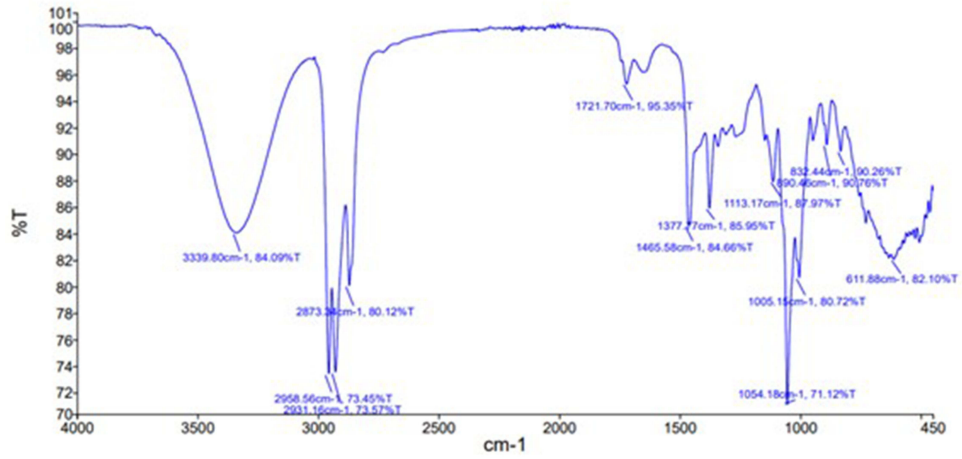

Figure 3 FTIR spectra of aqueous nanoparticles exhibited various peaks. The resultant peaks show that a variety of functional groups of bioactive substances are present. The aqueous extract of *T. vulgaris* nanoparticles FT-IR spectrum data showed that alkane (C-H) with a peak at 250 cm-^{1}, aromatic ester (C-O) with a peak at 1250 cm-^{1}, and alcohols (OH-) with a peak at 3363.6 cm-^{1}. The existence of hydroxyl and carbonyl groups was 2500–3300 cm-^{1} and 1680–1755 cm-^{1} respectively. Alcohols (OH-) have a peak in the FTIR analysis between 3700 and 3584 cm-^{1}. Amines (NH2), peaking between 1650 and 1580 cm-^{1}.

Zeta Potential

A sharp zeta potential was observed for AgNPs synthesized by biosynthesis (Figure 5). The zeta potentials of AgNPs in the aqueous extract were −7.46 ± 4.93 mV. AgNPs were dispersed in the medium due to their negative charge. When a particle's value is negative, it indicates that it is very stable and repels other particles.[35]

Size Distribution Analysis (Zeta Sizer)

In this study, AgNPs were measured using a dynamic light scattering technique extracted from the extracts of aqueous extracts from *T. vulgaris*. Figure 6 indicated in the histogram shows that the size of the AgNPs from *T. vulgaris* is 62.18 nm, and the average of AgNPs is 44.06 nm. The Pdi for the AGNPs was quite larger (0.260) which means that the distribution was broader, or the particle size distribution was multimodal.

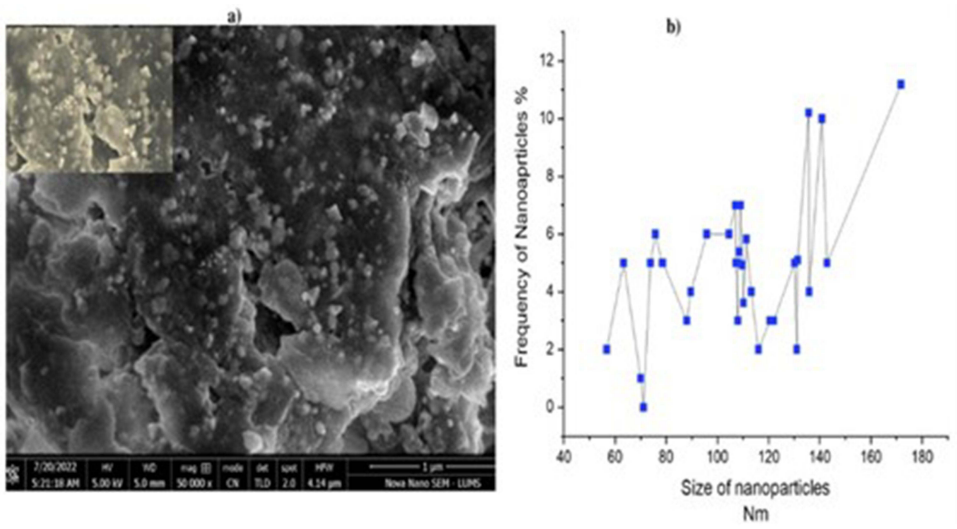

Figure 4 SEM analysis of silver nanoparticles at different magnification fig (**a**) shows the 2000,000 magnification of silver nanoparticle and fig (**b**) show the 50,000 magnifications.

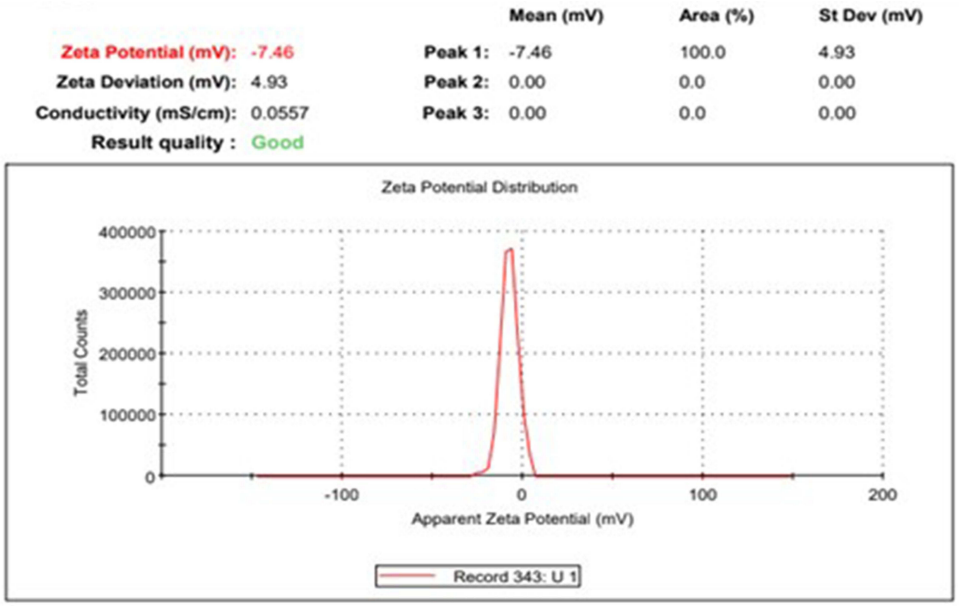

Figure 5 Zeta potential analysis of silver nanoparticles synthesized from *T. vulgaris* aqueous extract. A sharp zeta potential is observed.

X-Ray Diffraction (XRD) Analysis

The AgNPs were studied using X-ray diffraction in order to confirm their crystallinity. Silver exhibits a cubic structure with a face-centred cubic pattern in the XRD pattern. In the XRD spectrum, silver nanocrystals were observed in the form of nanocrystals as evidenced by the peaks at 2θ values of 25.33°, 27.92°,32.18°, 48.30° and 52.04° corresponding to (740), (642), (584), and (316). Hence, due to its face-centred cubic structure, silver may be indexed for Bragg reflections. *T. vulgaris* aqueous extract demonstrates by X-ray diffraction that AgNPs are crystalline after Ag^{+} ions are reduced by it as shown in Figure 7.

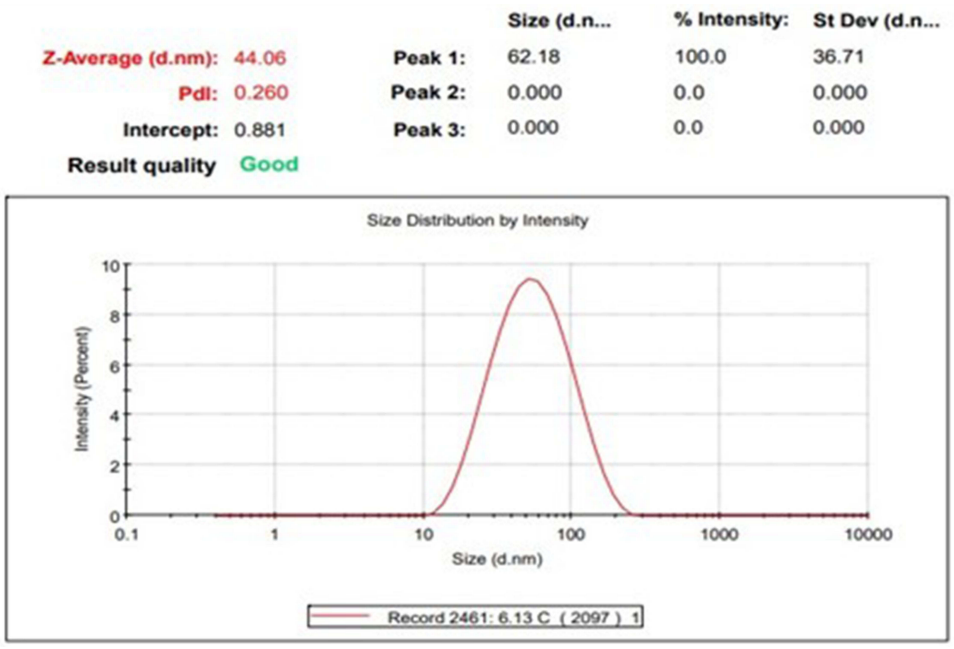

Figure 6 Size distributions analysis of silver nanoparticles synthesized from *T. vulgaris* aqueous extract. The histogram shows the size of the AgNPs from *T. vulgaris* is 62.18 nm and the average of AgNPs is 44.6 nm.

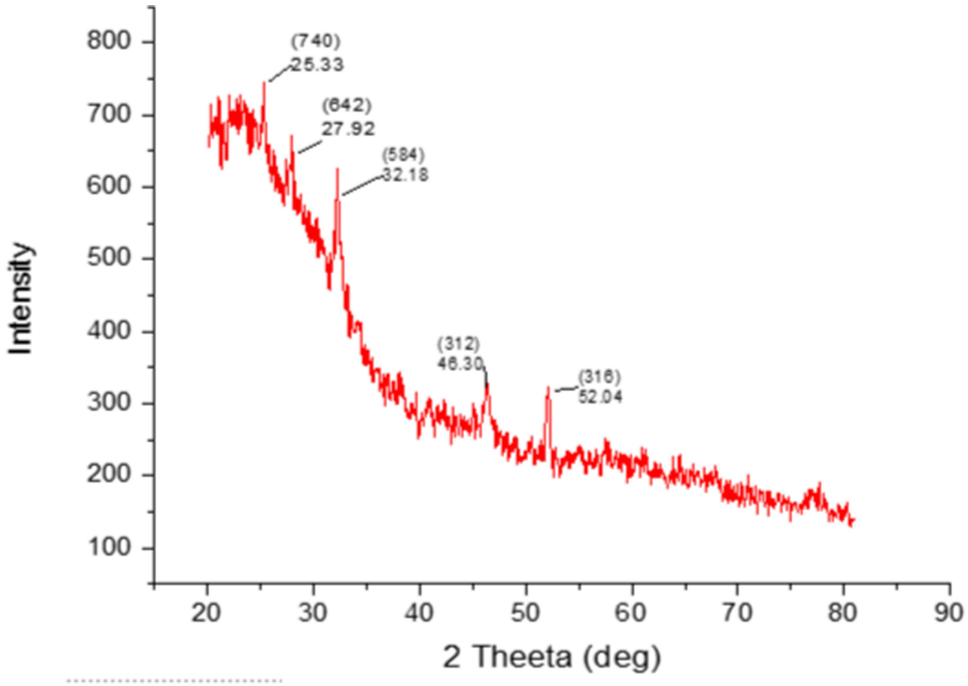

Figure 7 XRD analysis silver nanoparticles synthesis of *T. vulgaris* aqueous extract. The XRD spectrum shows that the silver nanocrystals were observed in the form of nanocrystals as evidenced by the peaks at 20 values of 25.33°, 27.92°,32.18°, 48.30° and 52.04° corresponding to (740), (642), (584), and (316).

Redox Parameters (kJ mol^{-1}) of Antioxidant Molecules

Using redox reactions, the antioxidant potentials of phenolics, R–OH (Caffeic acid, Sinapic acid, Gallic acid, and Benzoic acid) and flavonoids (Kaempferol, Myricetin, Quercetin) were assessed. In this study, we measured antioxidant

effects using three general mechanisms: single electron transfer followed by SET-PT, and HAT. When hydrogen is dissociated from phenolic compounds' active hydroxyl group, an electron is transferred from deprotonated molecules to the reduced ion/compound. SET-PT is a second reaction where electrons are transferred and the proton is detached. Another mechanism involves transferring hydrogen atoms directly from the antioxidant to the reduced substance (silver ions).[36] Aqueous plant extract contains AgNP, which can participate in redox reactions. As a result of hydrogen atoms reacting with carbon dioxide atoms in phenolic antioxidants, bond dissociation enthalpy is formed and provides the free Gibbs energy for the detachment of hydrogen atoms from the whole molecules as a consequence of the bond dissociation energy as shown in reaction 1.

(1) $R - OH = R - O \cdot + H$

PA (proton affinity) and ETE (electron transfer enthalpy) parameters describe two consecutive SPLET reactions. Reactions 2 and 3, which involve the hydroxyl group of the phenol compound being dissociated and the subsequent detachment of an electron from the R-O-anion, respectively, and reactions 2, which involve the hydroxyl group of the phenol compound being dissociated and the detachment of an electron from the R-O-anion:

1. (2) $R - OH = R - O$
2. (3) $R - O^{-} = R - O\cdot + e$

A procedure for identifying and calculating ETE values for compounds with multiple active hydroxyl groups (such as those with the lowest PA value) was used for phenolic compounds with several active hydroxyl groups. The PDE value (proton dissociation enthalpy) of SET-PT reactions is calculated from the IP value. Reaction 4 determines the adiabatic ionization energy and reaction 5 determines the proton dissociation enthalpy (reactions 5):

1. (4) $R - OH = R - OH$
2. (5) $R - OH^{+} = R - O + H^{+}$

The acceptable values for the group of antioxidants/reducing agents found in the aqueous extract of *T. vulgaris* are shown in Table 3.

Antioxidant Activity (2, 2-Diphenyl-1-Picrylhydrazyl (DPPH)

DPPH radical scavenging activity was demonstrated by using the biosynthesized AgNPs and plant extracts. Additionally, the results demonstrated that the antioxidant activity of AgNPs, plant extracts, and ascorbic acid is dose-dependent since the DPPH scavenging properties increased in percentage with increasing concentrations (250 g to 1000 µg) (Figure 8). Comparing AgNPs with plant extracts, AgNPs displayed an efficient DPPH scavenging ability. Vitamin C also exhibited an antioxidant effect. AgNPs have an antioxidant activity of 95.46%, whereas vitamin C has an antioxidant activity of 94.46%. In comparison with ascorbic acid, AgNPs displayed greater antioxidant activity.

Table 3 Redox Conditions for Antioxidant Molecules in the Proton Transfer and Hydrogen Atom Transfer Pathways (kJ mol^{-1})

Serial Number	Molecules	Proton Affinity	BDE values	Activity of O Group
1	Gallic acid	363.95	−4.40	11-O
2	Chlorogenic acid	351.40	−4.94	24-O
3	Caffeic acid	370.22	−5.19	12-O
4	Quercetin	357.67	−4.12	19-O

Abbreviation: BDE, Bond dissociation enthalpy.

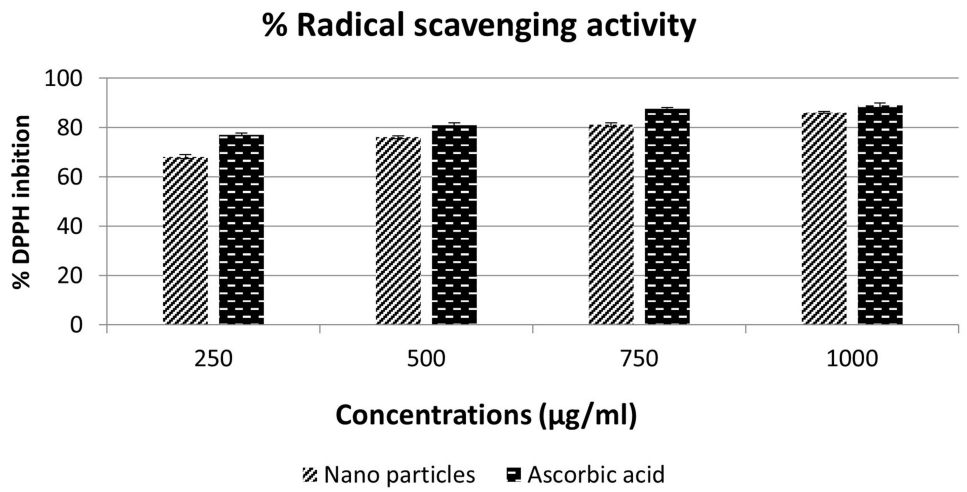

Figure 8 Represents the percentage of Antioxidant (DPPH). Values are mean ±S.D; data represented in triplicate.

Anti-Diabetic Activity

An increase in inhibitory activity against the alpha-amylase enzyme was observed as a result of dose-dependent activity. Using synthesized AgNPs, inhibitory activity was observed from 50.67% to 82.57% at concentrations of 250–1000 µg/mL (Figure 9). Metformin is a standard drug for α-amylase inhibitors which showed α-amylase inhibitory activity from 53.57 to 85.77% at the same concentrations. A greater inhibitory effect is observed with synthesized AgNPs than with standard AgNPs.

Hemolytic Activity

Concentration was a determinant of hemolysis activity after hemolysis activity was performed. In Figure 10, maximum hemolysis was achieved by using 1000 µg/mL (9.6) at the highest concentration. All lower concentrations of the compound exhibited less than 10% hemolytic activity, which is considered safe for use.[35] Despite low concentrations of hemolysis activity, NPs at low concentrations proved not to be toxic or biocompatible.

In-Vitro Anti-Inflammatory Activity

In this analysis, the anti-inflammatory efficacy was evaluated at four separate reaction mixture concentrations of 250 (µg/mL), 500 (µg/mL), 750 (µg/mL) and 1000 (µg/mL) which is shown in Figure 11. Anti-inflammatory activity with

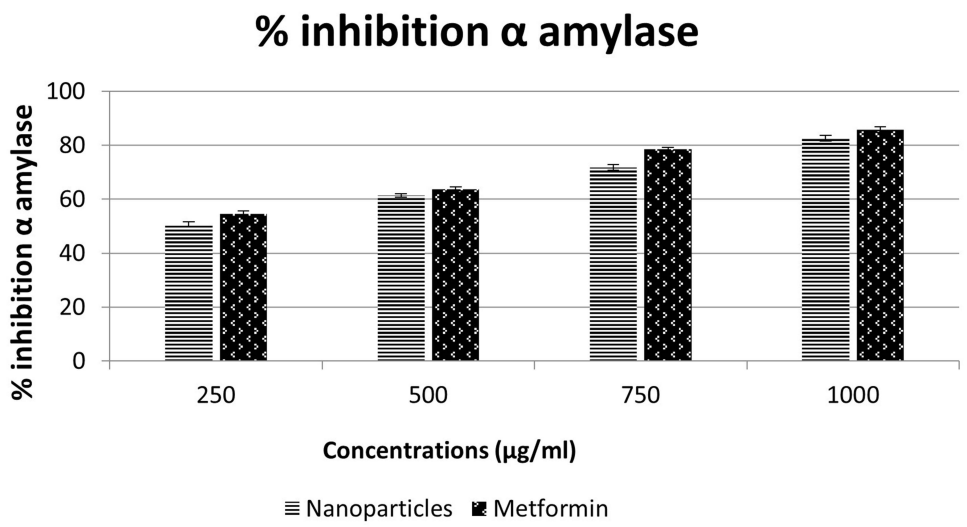

Figure 9 Antidiabetic potential (% inhibition) of Nanoparticles of *Thymus vulgaris*. Vertical bar represents the standard error with p >0.005.

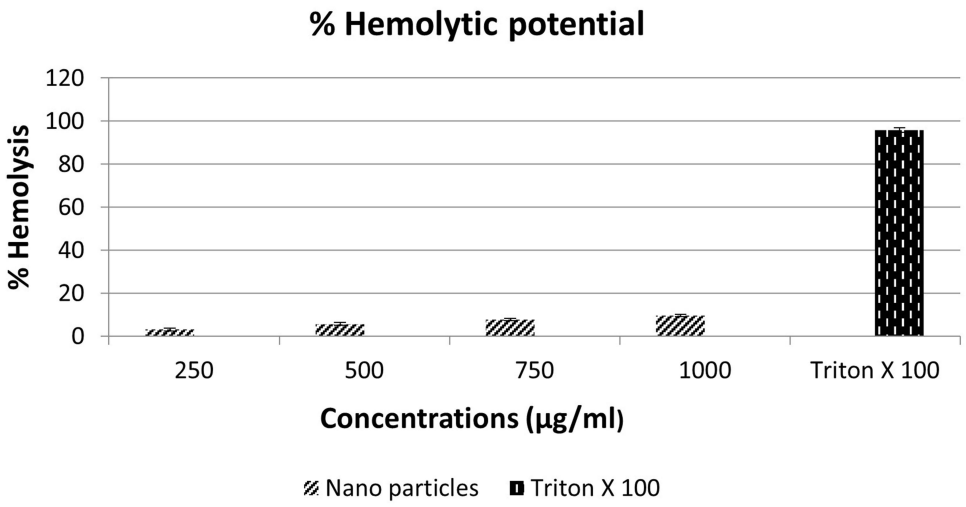

Figure 10 Percentage (%) hemolytic effect of nanoparticles of *Thymus vulgaris*. Values are mean ±S.D; data represented in triplicate.

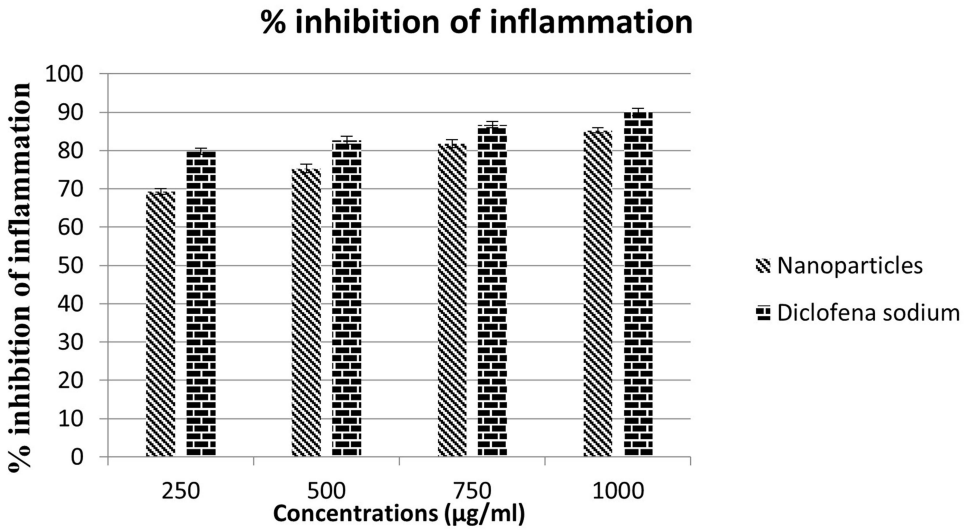

Figure 11 % denaturation of protein inhibition of silver nanoparticles *T. vulgaris*. Values are mean ±S.D; data represented in triplicate.

varying inhibition percentages, such as 69%, 75%, 83% and 85%. At 1000 µg/mL, the biogenerated nanosilver inhibits protein denaturation by 85%, which indicates its ability to prevent inflammatory proteins from being denatured.

In-Vivo Anti-Inflammatory Activity

In Table 4, biogenic AgNPs reduce the size of the edema in rats induced by carrageenan. Specific edema is produced within 30 minutes after injection of carrageenan. Approximately 30 minutes after injection, this edema begins to escalate and reaches its peak after three hours. In comparison with the control group, AgNPs significantly decreased paw edema after oral administration. A maximum inhibition percentage of 75.64% was obtained for the doses of 250,500,750, and 1000 (ug/mL) (body weight), respectively, after one hour, 87.21% after five hours, 88.54% after five hours, and 92.16% after five hours. Carrageenan-induced paw edema was significantly reduced by 71.50% by diclofenac sodium tested as a standard drug (p = 0.001). At 1 hour, inflammation occurs, while at 1000 grams, high doses are used to treat inflammation.

Table 4 *In-Vivo* Anti-Inflammatory Potential of Nanoparticles of *Thymus vulgaris*

Group	Dose (mg/kg Body Weight)	Paw size (mm) Mean ± S.D					% Inhibition of 3rd Hour
		0 Hour	1st Hour	2nd Hour	3rd Hour	4th Hour	
Control (Normal Saline)	250	3.55±0.033	3.78±0.11	3.86±0.04	3.99±0.023	3.98±0.033	–
	500	62±0.042	3.79±0.13	3.85±0.02	95±0.053	90±0.043	
	750	94±0.023	3.35±0.04	3.78±0.01	87±0.093	89±0.053	
	1000	32±0.05	3.48±0.02	3.52±0.05	88±0.11	80±0.14	
Diclofenac sodium (10 mg/kg) (Standard)	250	2.51±0.03	1.96±0.01	1.71±0.03	1.52±0.03	1.50±0.03	61.90%
	500	2.09±0.04	1.45±0.02	1.39±0.31	1.29±0.04	1.20±0.04	67.34%
	750	1.90±0.03	1.26±0.09	1.09±0.21	0.96±0.13	0.94±0.02	75.19%
	1000	1.59±0.45	0.96±0.04	0.81±0.04	0.70±0.31	0.61±0.04	81.95%
Nanoparticles	250	2.40±0.03	2.00±0.04	1.85±0.03	1.67±0.03	1.60±0.03	58.14%
	500	2.00±0.04	1.57±0.02	1.50±0.04	1.47±0.04	1.43±0.21	62.78%
	750	2.05±0.01	1.46±0.02	1.23±0.04	1.12±0.11	1.13±0.02	71.05%
	1000	1.89±0.02	1.35±0.04	1.12±0.02	0.88±0.02	0.89±0.03	77.31%

Discussion

Nanoparticles derived from biological processes are gaining importance day by day in nanoscience and can be used for a variety of medicinal applications. In recent years, novel nanotechnologies have gained enormous attention in the field of research as they exhibit vast applications in the multidisciplinary field. Different studies have shown the nutraceutical and pharmaceutical potential of NPs in which they interact with a high degree of sensitivity, specificity and signaling capability to the molecular as well as cellular level.[13] Despite the fact that NPs are used every day, their toxicity could be dangerous for human health. Therefore, more studies and evaluations are needed to keep developing and employing NPs.[37]

T. vulgaris contains a large number of biologically active compounds such as gallic acid, caffeic acid, chlorogenic acid, quercetin, xylitol and quinoline which were often considered to act as reducing agents in the green synthesis of silver ions.[15] Results of the current study showed that the aqueous plant extract *T. vulgaris* have quantity of phenolics and flavonoids. The highest quantified phenolics were caffeic acid followed by gallic acid and chlorogenic acid. Similar results have been seen in a previous study on *T. vulgaris* extracts which shows that the extracts contained at most phenolic and flavonoid compounds.[6] Other researchers also obtained similar results with phenolic and flavonoid compounds.[38]

In the current study, it was noted in the GC-MS analysis that a total of eight compounds consisting of 100% of the total compounds were detected. Furthermore, it was noticed that there's a much smaller energy required to transfer electrons from a deprotonated molecule than hydrogen, as shown in Table 1. It seems that HAT is the best redox process since atoms or electrons detach from molecules. Caffeic acid has the highest proton affinity 370.22 kJ mol^{-1} among phenolics as compared to quercetin which has the highest proton affinity 357.67 kJ mol^{-1} among flavonoids. Therefore, flavonoids can be expected to contribute a smaller amount to decrease the ability than phenolic compounds. Consequently, flavonoids and phenolic acid reactions are act as reducing agents which was similarly reported by Laguta et al.[3] Different compounds have a greater effect on HAT reactions than on SET-PT reactions. In comparison to other phenols, flavonoids are often regarded as having greater antioxidant properties as well as reducing properties.[39]

Green synthesis of NPs exhibits an advantage over the conventional method as it is clean, cost-effective, and gives results in an excellent manner. Multiple characterization methods have been performed for the validation of the aq. NPs. In the current study, the synthesized NPs were confirmed by UV–visible spectroscopy at approximately of 400 nm wavelength. In UV–visible range, AgNPs exhibit a maximum absorption due to surface plasmon resonance between 400 and 500 nm. As a result, it was revealed that the form of AgNPs reduced by *T. vulgaris* extract was spherical and dispersed, indicating that the peak of absorption was narrow and a single peak resonance peak was also obtained from surface plasmon resonance peaks concentrated near 400 nm, confirmed that *T. vulgaris* extract reduces silver ions and converts them to AgNPs.

To characterize the shape of the AgNPs, the SEM analysis was performed which revealed that the AgNPs were primarily spherical in shape and size ranging between 45 and 165 nm as shown in the distribution graph of SEM. Furthermore, the FTIR spectroscopy was carried out to identify functional groups of aq. AgNPs and their effect as reducing and capping agents on the formation of AgNPs. Figure 4 shows that FTIR spectra of synthesized NPs in which the spectra at 2930.94 cm^{-1} and 1736.52 cm^{-1} belong to the OH and C=H stretches bonds group. In this study, to validate the stability of the AgNPs, the zeta potential analysis was performed and the result shows −7.46 ± 4.93 mV value which indicates that bio-functionalized AgNPs from aqueous extracts of *T. vulgaris* have greater stability.[19]

The zeta sizer was performed to analyze the size of the AgNPs which was 62.18 nm, while the average size of AgNP is 44.6 nm. The current results are in line with a previous study conducted which shows zeta sizer of *T. vulgaris* AgNPs 44.99 nm that reduced metal ions which lead to the formation of AgNPs with well-defined dimensions.[40] In the current study, the XRD spectrum revealed that the AgNPs have a nanocrystal nature, as evidenced by the peaks in the diffractogram. At 2θ values of 25.33°, 27.92°, 32.18°, 48.30° and 52.04° corresponding to (hkl) values (740), (642), (584), and (316) planes of AgNPs.

The synthesized NPs by using the green approach have the potential against different diseases. To explore the potential of biogenic synthesized NPs, different biological activities were performed. The antioxidant activity was performed as antioxidant scavenges the harmful free radicals from the body and reduces the risk of damage caused by the oxidation process. Phenolics and flavonoids are strong antioxidants and act as a binding molecule in the synthesis of NPs which may increase their efficiency and effectivity. The antioxidant activity of biogenic AgNPs was performed using DPPH as an oxidant, and the result revealed that AgNPs at different concentrations of 250 µg/mL (77.2%), 500 µg (81.0%), 750 µg (87.9%), 1000 µg (89.0%) exhibits good potential as an antioxidant. The AgNPs have high catalytical potential, along with a strong adsorption ability and low toxicity; therefore, they have excellent bioavailability.[13] A comparison of alpha-amylase inhibitory properties of NPs in-vitro is shown in Figure (10). An increase in inhibitory activity against the alpha-amylase enzyme is observed in a dose-dependent manner. Using concentrations of 250–1000 µg/mL (Figure 9), AgNPs showed inhibitory activity of 50.67% to 82.57%. Using the same concentrations, metformin was found to inhibit amylase from 53.57% to 85.77%. Synthesized AgNPs showed better inhibitory effects than the standard when compared to the standard. Aq. NPs must be studied in-depth in terms of in-vitro procedures in order to establish them as a competitive option to treat type 2 diabetes mellitus.[28]

The hemolysis of RBCs was performed to measure the toxicity of biogenic NPs in which hemoglobin was released from RBCs through the rupture of their membrane. The abiogenic NPs have more toxicity as compared to biogenic NPs. The AgNPs are crucial in studying hemolysis; thus, it is essential to study hemolytic effects. The safe range for hemolytic activity is less than 10%.[32] The hemolytic activity was performed for optimized NPs at different concentrations among which 1000 µg/mL shows the highest hemolytic activity at 9.66% (RBC) lysis and lowest at 250 µg/mL concentration shows 3% lysis to assess the toxic effect of AgNPs. The current study was also supported by.[41] As AgNPs concentrations increased, a high degree of hemolytic activity was observed, indicating that AgNPs toxicity is concentration-dependent, furthermore, from the current study it is inferred that less than 1000 ug/mL concentration of biogenic NPs might be used to cure health hazards.

The AgNPs synthesized in an environmentally friendly manner by using *T. vulgaris* aqueous extract and have natural anti-inflammatory effects. In the present study, as for anti-inflammatory activity, AgNPs showed the greatest percentage of inhibition against BSA protein at 1000 µg/mL (85%) and the lowest activity at 250 µg/mL (69%). In an *in-vivo* study of rats with carrageenan-induced hind paw edema, AgNPs powered by an aqueous extract of *T. vulgaris* were tested for their anti-inflammatory properties. In spite of its wide use, the model has a high reproducibility and is widely used in the study of acute inflammation. As a result of the persistence of the anti-inflammatory effects, the absence of paw edema occurred only in the third phase (p-0.005). Those results are similar to those obtained in the reported study.[33]

Conclusion

Nanotechnology is the most important field for developing new medical applications. The present investigation is highly necessitated to throw more light upon the AgNPs synthesized from *T. vulgaris* aqueous extract. From the present study, it was concluded that the characterization of AgNPs using UV–vis spectra confirms the formation of green synthesized AgNPs at 400 nm wavelength. FTIR spectra revealed the phytochemicals which may reduce and cap AgNPs. Furthermore, the SEM analysis, zeta potential, and zeta sizer analysis on AgNPs validated the shape, size and stability

of biogenic AgNPs. In addition, the AgNPs at different quantum calculation analysis depicted that plant-based bioactive compounds are having greater antioxidant properties, as well as reducing properties. Therefore, it was confirmed that AgNPs synthesized from *T. vulgaris* aqueous extract can be a good source of natural medicinal plants with antioxidant, antidiabetic, and anti-inflammatory potentials.

Institutional Review Board Statement

The animal study was reviewed and approved by Institutional Review Board (IRB), Research Ethics Committee, University of Central Punjab (protocol code: CP/FOLS/210419-7/1-Animal, approved on 21 April 2021). While the study involving human participants were reviewed and approved with protocol code: CP/FOLS/210419-7/1-Human, approved on 21 April 2021. The patients/participants provided their written informed consent to participate in this study. The study was performed in accordance with relevant institutional and national guidelines and regulations. For the animal study, the International Association of Veterinary Editors (AVMA) guidelines were followed.

Acknowledgments

This research work was supported by Institutional Fund Project under grant no. (IFPIP: 1639-166-1443). The authors gratefully acknowledge technical and financial support provided by the Ministry of Education and King Abdulaziz University, DSR, Jeddah, Saudi Arabia. Furthermore, the author acknowledges the University of Central Punjab for providing the research facilities. Naveed Ahmed would like to acknowledge graduate research assistance scheme of Universiti Sains Malaysia.

Disclosure

The authors report no conflicts of interest in this work.

References

1. Batool S, Hussain Z, Niazi MBK, Liaqat U, Afzal M. Biogenic synthesis of silver nanoparticles and evaluation of physical and antimicrobial properties of Ag/PVA/starch nanocomposites hydrogel membranes for wound dressing application. *J Drug Delivery Sci Technol*. 2019;52:403–414. doi:10.1016/j.jddst.2019.05.016
2. Sharifi-Rad M, Pohl P, Epifano F, Álvarez-Suarez JM. Green synthesis of silver nanoparticles using Astragalus tribuloides delile root extract: characterization, antioxidant, antibacterial, and anti-inflammatory activities. *Nanomaterials*. 2020;10(12):2383. doi:10.3390/nano10122383
3. Laguta I, Stavinskaya O, Kazakova O, Fesenko T, Brychka S. Green synthesis of silver nanoparticles using Stevia leaves extracts. *Appl Nanosci*. 2019;9(5):755–765. doi:10.1007/s13204-018-0680-5
4. Sim S, Wong NK. Nanotechnology and its use in imaging and drug delivery. *Biomed Rep*. 2021;14(5):1–9. doi:10.3892/br.2021.1418
5. Pirtarighat S, Ghannadnia M, Baghshahi S. Green synthesis of silver nanoparticles using the plant extract of Salvia spinosa grown in vitro and their antibacterial activity assessment. *J Nanostruct Chem*. 2019;9(1):1–9. doi:10.1007/s40097-018-0291-4
6. Balciunaitiene A, Viskelis P, Viskelis J, et al. Green synthesis of silver nanoparticles using extract of Artemisia *absinthium* L, *Humulus lupulus* L. and *Thymus vulgaris* L, Physico-Chemical Characterization, Antimicrobial and Antioxidant Activity. *Processes*. 2021;9(8):1304. doi:10.3390/pr9081304
7. Suman TY, Rajasree SR, Jayaseelan C, et al. GC-MS analysis of bioactive components and biosynthesis of silver nanoparticles using Hybanthus enneaspermus at room temperature evaluation of their stability and its larvicidal activity. *Environ Sci Pollut Res Int*. 2016;23(3):2705–2714. doi:10.1007/s11356-015-5468-5
8. Hembram KC, Kumar R, Kandha L, Parhi PK, Kundu CN, Bindhani BK. Therapeutic prospective of plant-induced silver nanoparticles: application as antimicrobial and anticancer agent. *Artif Cells Nanomed Biotechnol*. 2018;46(sup3):38–51. doi:10.1080/21691401.2018.1489262
9. Abdellatif AAH, Alhathloul SS, Aljohani ASM, et al. Green synthesis of silver nanoparticles incorporated aromatherapies utilized for their antioxidant and antimicrobial activities against some clinical bacterial isolates. *Bioinorg Chem Appl*. 2022;2022:2432758. doi:10.1155/2022/2432758
10. Jadou A, Al-Shahwany AW. Biogenic synthesis and characterization of silver nanoparticles using some medical plants and evaluation of their antibacterial and toxicity potential. *J AOAC Int*. 2018;101(6):1905–1912. doi:10.5740/jaoacint.17-0500
11. Khanal LN, Sharma KR, Paudyal H, et al. Green synthesis of silver nanoparticles from root extracts of Rubus ellipticus Sm and comparison of antioxidant and antibacterial activity. *J Nanomater*. 2022;2022:1–11. doi:10.1155/2022/1832587
12. Kedi PBE, Meva FE, Kotsedi L, et al. Eco-friendly synthesis, characterization, in vitro and in vivo anti-inflammatory activity of silver nanoparticle-mediated Selaginella myosurus aqueous extract. *Int J Nanomed*. 2018;13:8537–8548. doi:10.2147/IJN.S174530
13. Pandiyan I, Sri SD, Indiran MA, Rathinavelu PK, Prabakar J, Rajeshkumar S. Antioxidant, anti-inflammatory activity of Thymus vulgaris-mediated selenium nanoparticles: an in vitro study. *J conservat Dent*. 2022;25(3):241–245. doi:10.4103/JCD.JCD_369_21
14. Aldosary S, El-Rahman S, Al-Jameel S, Alromihi N. Antioxidant and antimicrobial activities of Thymus vulgaris essential oil contained and synthesis thymus (Vulgaris) silver nanoparticles. *Braz J Biol*. 2021;3:83.
15. Khalilnezhad F, Torabi S, Larijany K, Khosrowshahli M. Nano silver particle synthesis using leaf extract of pharmaceutical plant Thymus vulgaris. *Int J Biosci*. 2015;6(4):192–196.
16. Mohammadi M, Shahisaraee SA, Tavajjohi A, et al. Green synthesis of silver nanoparticles using Zingiber officinale and Thymus vulgaris extracts: characterisation, cell cytotoxicity, and its antifungal activity against Candida albicans in comparison to fluconazole. *IET Nanobiotechnol*. 2019;13(2):114–119. doi:10.1049/iet-nbt.2018.5146

17. Odemis O, Ozdemir S, Gonca S, Arslantas A, Agirtas MS. The study on biological activities of silver nanoparticles produced via green synthesis method using Salvia officinalis and Thymus vulgaris. *Turk J Chem*. 2022;46(5):1417–1428. doi:10.55730/1300-0527.3448
18. De Melo APZ, De Oliveira Brisola Maciel MV, Sganzerla WG, et al. Antibacterial activity, morphology, and physicochemical stability of biosynthesized silver nanoparticles using thyme (Thymus vulgaris) essential oil. *Mater Res Express*. 2020;7(1):015087. doi:10.1088/2053-1591/ab6c63
19. Heidari Z, Salehzadeh A, Sadat Shandiz SA, Tajdoost S. Anti-cancer and anti-oxidant properties of ethanolic leaf extract of Thymus vulgaris and its bio-functionalized silver nanoparticles. *3 Biotech*. 2018;8(3):1–14. doi:10.1007/s13205-018-1199-x
20. Deshmukh MM, Ambad CS, Kendre N, Kashid NG. Biochemical Screening, Antibacterial and GC-MS Analysis of Ethanolic Extract of *Hemidesmus indicus* (L) R. Br. root. *Res J Pharma Phytochem*. 2019;11(2):73–80. doi:10.5958/0975-4385.2019.00014.1
21. Banerjee P, Satapathy M, Mukhopahayay A, Das P. Leaf extract mediated green synthesis of silver nanoparticles from widely available Indian plants: synthesis, characterization, antimicrobial property and toxicity analysis. *Bioresou Biopro*. 2014;1(1):1–10. doi:10.1186/s40643-014-0003-y
22. Vignesh A, Selvakumar S, Vasanth K. Comparative LC-MS analysis of bioactive compounds, antioxidants and antibacterial activity from leaf and callus extracts of *Saraca asoca*. *Phytomedicine Plus*. 2022;2(1):1–12. doi:10.1016/j.phyplu.2021.100167
23. Afzal M, Khan AS, Zeshan B, et al. Characterization of bioactive compounds and novel proteins derived from promising source Citrullus *colocynthis* along with in-vitro and in-vivo activities. *Molecules*. 2023;28(4):1743. doi:10.3390/molecules28041743
24. Kostikova VA, Veklich TN HPLC analysis of phenolic compounds in leaves and inflorescences of Sorbaria pallasii. Paper presented at: BIO Web of Conferences; 2020.
25. Filip GA, Moldovan B, Baldea I, et al. UV-light mediated green synthesis of silver and gold nanoparticles using Cornelian cherry fruit extract and their comparative effects in experimental inflammation. *J Photochem Photobiol B Biol*. 2019;191:26–37. doi:10.1016/j.jphotobiol.2018.12.006
26. Khyade MS, Varpe SN, Padwal AD. Evaluation of chemical profile and antioxidant potential of Trichodesma indicum (L.) R. Br. *Int J Phytomed*. 2017;9(3):416–425. doi:10.5138/09750185.2012
27. Chand K, Cao D, Eldin Fouad D, et al. Green synthesis, characterization and photocatalytic application of silver nanoparticles synthesized by various plant extracts. *Arabian J Chem*. 2020;13(11):8248–8261. doi:10.1016/j.arabjc.2020.01.009
28. Perumalsamy R, Krishnadhas L. Anti-Diabetic Activity of Silver Nanoparticles Synthesized from the Hydroethanolic Extract of Myristica fragrans Seeds. *Appl Biochem Biotechnol*. 2022;194(3):1136–1148. doi:10.1007/s12010-022-03825-8
29. Erdogan O, Abbak M, Demirbolat GM, Birtekocak F. Green synthesis of silver nanoparticles via Cynara scolymus leaf extracts: the characterization, anticancer potential with photodynamic therapy in MCF7 cells. *PLoS One*. 2019;14(6):e0216496. doi:10.1371/journal.pone.0216496
30. Keshari AK, Srivastava R, Singh P, Yadav VB, Nath G. Antioxidant and antibacterial activity of silver nanoparticles synthesized by Cestrum nocturnum. *J Ayurveda Integr Med*. 2020;11(1):37–44. doi:10.1016/j.jaim.2017.11.003
31. Chahardoli A, Qalekhani F, Shokoohinia Y, Fattahi A. Biological and catalytic activities of green synthesized silver nanoparticles from the leaf infusion of Dracocephalum kotschyi boiss. *Global Challenges*. 2021;5(2):2000018. doi:10.1002/gch2.202000018
32. Saleem A, Afzal M, Naveed M, et al. HPLC, FTIR and GC-MS analyses of thymus vulgaris phytochemicals executing in vitro and in vivo biological activities and effects on COX-1, COX-2 and gastric cancer genes computationally. *Molecules*. 2022;27(23):8512. doi:10.3390/molecules27238512
33. Das M, Mondal A, Patowary K, Malipeddi H. Biosynthesis of AgNPs using aqueous leaf extract of Ipomoea eriocarpa and their anti-inflammatory effect on carrageenan-induced paw edema in male Wistar rats. *IET Nanobiotechnol*. 2017;11(3):225–229. doi:10.1049/iet-nbt.2016.0034
34. Vanaja M, Gnanajobitha D, Paulkumar K, Shanmugam R, Chelladurai M, Gurusamy A. Phytosynthesis of silver nanoparticles by 'Cissus quadrangularis', influence of physicochemical factors. *J Nanostruct Chem*. 2013;3:3.
35. Anandalakshmi K, Venugobal J, Ramasamy V. Characterization of silver nanoparticles by green synthesis method using Pedalium murex leaf extract and their antibacterial activity. *Appl Nanosci*. 2016;6(3):399–408. doi:10.1007/s13204-015-0449-z
36. Litwinienko G, Ingold K. Solvent effects on the rates and mechanisms of reaction of phenols with free radicals. *Acc Chem Res*. 2007;40(3):222–230. doi:10.1021/ar0682029
37. Fabara A, Cuesta S, Pilaquinga F, Meneses L. Computational modeling of the interaction of silver nanoparticles with the lipid layer of the skin. *J Nanotechnol*. 2018;2018:4927017. doi:10.1155/2018/4927017
38. Habashy NH, Serie MMA, Attia WE, Abdelgaleil SA. Chemical characterization, antioxidant and anti-inflammatory properties of Greek Thymus vulgaris extracts and their possible synergism with Egyptian Chlorella vulgaris. *Journal of Functional Foods*. 2018;40:317–328. doi:10.1016/j.jff.2017.11.022
39. Rice-Evans CA, Miller NJ, Paganga G. Structure-antioxidant activity relationships of flavonoids and phenolic acids. *Free Radic Biol Med*. 1996;20(7):933–956. doi:10.1016/0891-5849(95)02227-9
40. Tseng K-H, Chou C-J, Liu T-C, Tien D-C, Chang CY, Stobinski L. Relationship between Ag nanoparticles and Ag ions prepared by arc discharge method. *Nanotechnol Rev*. 2018;7(1):1–9. doi:10.1515/ntrev-2017-0167
41. Raja A, Salique SM, Gajalakshmi P, James A. Antibacterial and hemolytic activity of green silver nanoparticles from Catharanthus roseus. *Int J Pharm Sci Nanotechnol*. 2016;9(1):7.